Results in Physics 10 (2018) 164–172

Contents lists available at ScienceDirect

Results in Physics

journal homepage: www.elsevier.com/locate/rinp

Analytical solution of convective heat transfer of a quiescent fluid over a nonlinearly stretching surface using Homotopy Analysis Method

M.A. Kazemi[a,*], S.S. Jafari[b], S.M. Musavi[c], M. Nejati[d]

[a] Technical and Vocational University, Shahid Mofateh of Hamedan, Iran
[b] Young Researchers & Elite Club, Hamedan Branch, Islamic Azad University, Hamedan, Iran
[c] Mechanical Engineering Faculty, Tehran University, Tehran, Iran
[d] Young Researchers & Elite Club, Arak Branch, Islamic Azad University, Arak, Iran

ARTICLE INFO

Keywords:
Nonlinear stretching surface
Boundary layer
Thermal radiation
Similarity solution
Homotopy Analysis Method (HAM)

ABSTRACT

In this article, an analytical solution of the boundary layer fluid flow and heat transfer of a quiescent viscous fluid over a non-linearly stretching surface is presented. The thermal radiation effects are included in the energy governing equation. Surface velocity and temperature conditions are assumed to be of the power-law form with an exponent of 1/3 for velocity and arbitrary exponent m for surface temperature or heat flux conditions. The system of nonlinear differential equations is solved by Homotopy Analysis Method (HAM) for two cases of Prescribed Surface Temperature (PST) and Prescribed Heat Flux (PHF). The results of this method appear in the form of series expansions, the convergence of which is analyzed carefully. Graphical results are finally presented in order to investigate the influence of Prandtl number (Pr) and thermal radiation on heat transfer phenomena.

Introduction

A large number of engineering and scientific problems can be appropriately formulated in the form of a system of non-linear partial differential equations subject to specific boundary and initial conditions. However, a general methodology in order to analytically tackle with such systems of equations still lacks. The most common choice for complicated problems seems to be numerical computations, in which values of dependent variables are accounted for at only a set of discrete points (commonly referred to as computational nodes). Nevertheless, the analytical solutions are highly favored over numerical results especially because of their ability to continuously describe the variable fields and the lack of a number of errors that are typically associated with the numerical solutions.

There are many approximate analytical methods, which have been developed and extensively used for the case of ordinary non-linear differential equations. In the case of partial differential equations if a similarity variable exists, the system of differential equations is possible to be transformed to a system of ordinary differential equations. Then the analytical methods that are applicable to ODEs can be utilized in order to resolve the resulting system of ODEs.

There are many well-known method to solve equations such as DQ, GDQ, DTM and etc [1–4]. One of the most recently applied approximate analytical methods, for solving non-linear ordinary differential equations, is Homotopy Analysis Method (HAM), which was developed by Liao in 1992 [5]. It is the general form of HPM [6], ADM [7] and δ-expansion methods, which overcomes the restriction of requiring a small parameter in the foregoing methods [8]. In order to make sure about its validity and accuracy it was widely applied by many researchers for a variety of problems such as viscous boundary layer flow due to a moving sheet[9], viscos flow on flat plate [10], Blasius viscos flow [11], non-Newtonian fluids over a sheet [12], hydro magnetic nano-fluids [13], vibration of beams [14], boundary layer flows and heat transfer subject to non-linear boundary conditions [15–17].

Ajam et al. [18] applied Buongiorno's Model to study a surface stretching with convective conditions in a magnetohydrodynamic (MHD) nano-fluid. They showed by increasing Lewis number, the species boundary layer thins and the concentration profiles become steeper. Abbasbandy used Homotopy Analysis Method in many heat transfer problems such as heat radiation equations [19]. Marinca and Herişanu [20] investigated nonlinear equations arising in heat transfer bu OHAM. Sheikholeslami et al. [21] studied nanofluid flow over a stretching plate in existence of magnetic field by using Buongiorno Model. They showed by increasing porosity and melting parameters the Nusselt number reduced.

There are many industrial and chemical processes where a surface that is being stretched or drawn needs to be cooled before taking any further packaging or processing action. The cooling effect is typically

* Corresponding author.
E-mail address: m.a.kazemi@basu.ac.ir (M.A. Kazemi).

https://doi.org/10.1016/j.rinp.2018.05.036
Received 2 February 2018; Received in revised form 2 May 2018; Accepted 24 May 2018
Available online 30 May 2018

achieved by means of a fluid surrounding the surface, e.g. paper production, manufacturing electronic chips, iron forming, and many others. As of yet several engineering problems concerning stretching surfaces have been mathematically modeled under various conditions and using both Newtonian and non-Newtonian working fluids [22–27].

To name a few, heat transfer from a moving hot surface and nonlinear stretching effects on fluid flow were studied by Chen [28], and Vajravelu [29], respectively. Power law and exponentially stretching surface have been investigated by Ali [30] and Elbashbeshy [31], respectively. Cortell [32]conducted a numerical solution of the flow and heat transfer over a nonlinearly stretching sheet, using Runge-Kutta integration method.

In the present study, the system of non-linear equations of the fluid flow and heat transfer of a viscous quiescent fluid over a non-linearly stretching surface are analytically solved by HAM. The thermal radiation is also taken into account and the problem is solved subject to two sets of thermal boundary conditions, i.e., Prescribed Surface Temperature (PST) and Prescribed Heat Flux (PHF). The results showed that by increasing surface temperature parameter, dimensionless temperature in both PST and PHF cases decrease. Also dimensionless stream function, velocity and dimensionless temperature in both cases of PST and PHF are represented graphically.

Flow and energy analysis and mathematical formulation

Governing equations of fluid flow

As shown in Fig. 1, let us consider a Newtonian incompressible flow over a flat stretching surface which corresponds to $y = 0$ in the Cartesian coordinates system depicted. The surface is being stretched non-uniformly in x direction. The 2-dimensional constant-property boundary layer equations are expressed as Eqs. (1) and (2), which are the statements of conservation of mass and linear momentum in x direction, respectively. These governing equations are subject to the assumption of slender boundary layer which holds true for the case of high Re numbers ($Re = \overline{u}_w L/\nu$). The main consequences of slenderness assumption are $v \ll u$ and $\partial^2 u/\partial x^2 \ll \partial^2 u/\partial y^2$.

$$\frac{\partial u}{\partial x} + \frac{\partial v}{\partial y} = 0, \tag{1}$$

$$u\frac{\partial u}{\partial x} + v\frac{\partial u}{\partial y} = \nu\frac{\partial^2 u}{\partial y^2}. \tag{2}$$

Boundary conditions for the present problem as set forth by Cortell [32], are

$$u_w(x) = \frac{\nu}{L^{4/3}}x^{1/3}, \quad v = 0 \ at \ y = 0, \tag{3}$$

$$u \to 0 \quad as \quad y \to \infty. \tag{4}$$

In which L is the characteristic length of the surface taken as the streamwise surface extent. As noticed the wall stretching velocity appears as a nonlinear boundary condition, Eq. (3). Similarity variables are defined as follows [32]:

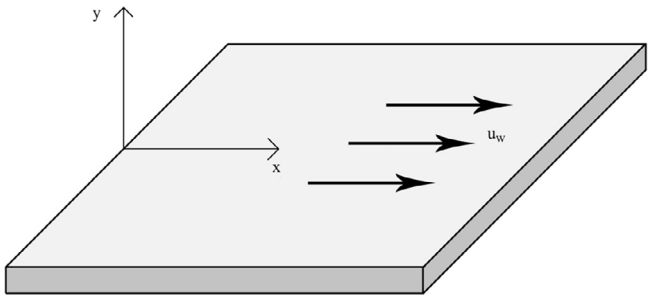

Fig. 1. The stretching surface, with surface velocity u_w.

$$\eta = y\frac{x^{-1/3}}{L^{2/3}}, \quad u = \frac{\nu}{L^{4/3}}x^{1/3}f'(\eta), \quad v = -\frac{\nu}{L^{2/3}}x^{-1/3}\frac{2f-\eta f'}{3}. \tag{5}$$

Eq. (2) is reduced to the following nonlinear differential equation [32]

$$3f''' + 2ff'' - (f')^2 = 0, \tag{6}$$

where f is the dimensionless stream function and the primes denote differentiation with respect to the similarity variable, η. The Eq. (6) is subject to boundary conditions given below:

$$f = 0, \quad f' = 1 \ at \ \eta = 0, \tag{7}$$

$$f \to 0 \quad as \quad \eta \to \infty. \tag{8}$$

Governing equation of heat transfer

The boundary layer including thermal radiation is given by Eq. (9) as

$$u\frac{\partial T}{\partial x} + v\frac{\partial T}{\partial y} = \alpha\frac{\partial^2 T}{\partial y^2} - \frac{1}{\rho C_p}\frac{\partial q_r}{\partial y}. \tag{9}$$

In which T is temperature, α the thermal diffusivity, ρ the fluid density, C_p is the fluid specific heat at constant pressure, and q_r is the radiative heat flux. Using Rosseland approximation [33] the radiative heat flux is simply expressed as follows:

$$q_r = -\frac{4\sigma}{3k^*}\frac{\partial T^4}{\partial y}, \tag{10}$$

where σ is the Stefan-Boltzmann constant and k^* is the mean absorption coefficient. By expanding T^4 using a Taylor series about T_∞ and neglecting higher-order terms Eq. (10) is simplified and then substituted in Eq. (9). Thus, the energy equation takes the following form of [32]:

$$u\frac{\partial T}{\partial x} + v\frac{\partial T}{\partial y} = \left(\alpha + \frac{16PrT_\infty^3}{3\rho C_p k^*}\right)\frac{\partial^2 T}{\partial y^2}. \tag{11}$$

Prescribed surface temperature (PST) case

The nonlinear boundary condition for surface temperature is considered as follows, with $m \neq 0$ and $m \neq 1$:

$$T_w = T_\infty + A\left(\frac{x}{L}\right)^m \ at \ y = 0, \quad T \to T_\infty \ as \ y \to \infty, \tag{12}$$

where A is a constant, and T_∞ is the free stream fluid temperature. For convenience the dimensionless temperature θ is defines as

$$\theta(\eta) = \frac{T - T_\infty}{T_w - T_\infty}. \tag{13}$$

Using similarity variable the Eqs. (11) and (12) are reduced to [32]:

$$\theta'' + \frac{2k_0}{3}Prf\theta' - Prk_0 mf'\theta = 0, \tag{14}$$

$$\theta = 1 \quad at \quad \eta = 0; \theta \to 0 \quad as \quad \eta \to \infty. \tag{15}$$

In which $Pr(=\nu/\alpha)$ is the fluid Prandtl number, $N_R = k^*k/4\sigma$ the radiation parameter [32], and we also have $k_0 = 3N_R/(3N_R + 4)$.

Prescribed heat flux (PHF) case

In this case, dimensionless temperature is defined as [32]

$$g(\eta) = \frac{T - T_\infty}{\left(\frac{D}{k}\right)x^{m+1/3}L^{2/3-m}}, \tag{16}$$

and the corresponding boundary conditions are

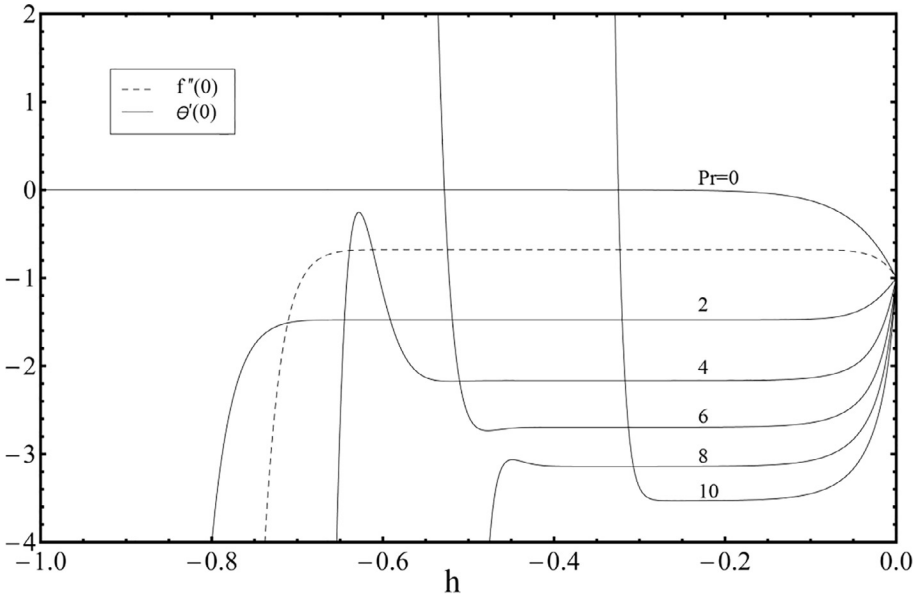

Fig. 2. The h-curves of $f''(0)$ and $\theta'(0)$ for several values of Prandtl number as obtained using the twentieth-order approximation of the HAM, for $k_0 = 1$ and $m = 1$.

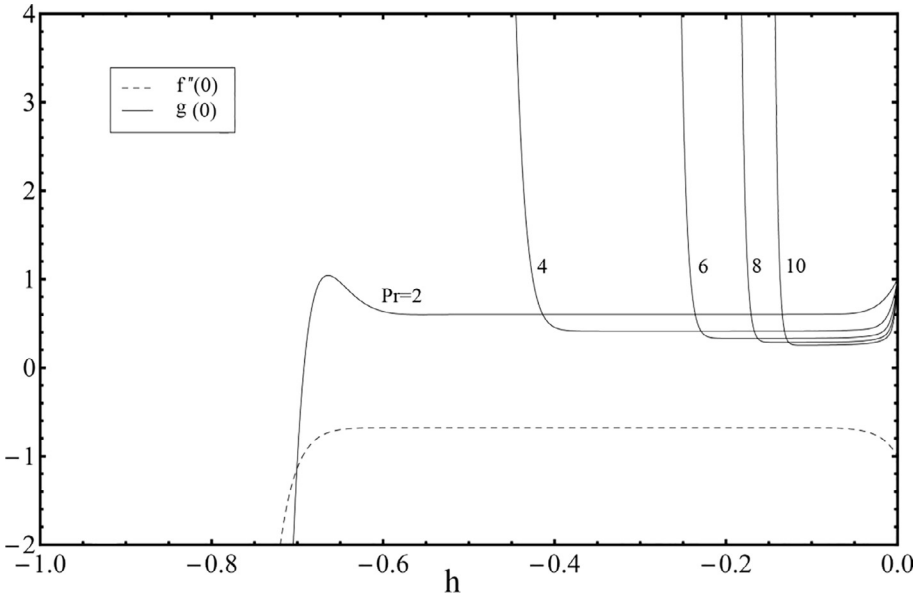

Fig. 3. The h-curves of $f''(0)$ and $g(0)$ for several values of Prandtl number as obtained using the twentieth-order approximation of the HAM, when $k_0 = 1$ and $m = 1$.

$$q_w = -k\left(\frac{\partial T}{\partial y}\right)_w = D\left(\frac{x}{L}\right)^m \quad at \quad y = 0, \ T \to T_\infty \quad as \quad y \to \infty, \tag{17}$$

where D is a constant and provided that $m \neq 0$ and $m \neq 1$ the wall heat flux turns out to be a nonlinear boundary condition. By using similarity transformations and Eqs. (16), (11) and (17) are reduced to [32]:

$$g'' + \frac{2k_0}{3}Prfg' - Prk_0\left(m + \frac{1}{3}\right)f'\theta = 0, \tag{18}$$

$$g' = -1 \quad at \quad \eta = 0; g \to 0 \quad as \quad \eta \to \infty. \tag{19}$$

HAM solution

To solve Eqs. (7), (14) and (18) analytically by using HAM, we choose the initial solutions as

$$f_0(\eta) = 1 - e^{-\eta}, \tag{20}$$

$$\theta_0(\eta) = e^{-\eta}, \tag{21}$$

$$g_0(\eta) = e^{-\eta}, \tag{22}$$

where Eqs. (20)–(22) satisfy the boundary conditions in (8), (15) and (19), respectively. Auxiliary linear operators are defined as

$$L_1(\eta) = f''' - f', \tag{23}$$

$$L_2(\eta) = \theta'' + \theta', \tag{24}$$

$$L_3(\eta) = g'' + g'. \tag{25}$$

These linear operators possess the following properties

$$\begin{aligned} &L_1(C_1 + C_2e^{-\eta} + C_3e^{\eta}) = 0, \\ &L_2(C_4 + C_5e^{-\eta}) = 0, \\ &L_3(C_6 + C_7e^{-\eta}) = 0, \end{aligned} \tag{26}$$

where C_i, $(i = 1–7)$ are integration constants. From Eqs. (7), (14) and (18) the nonlinear operators are defined as

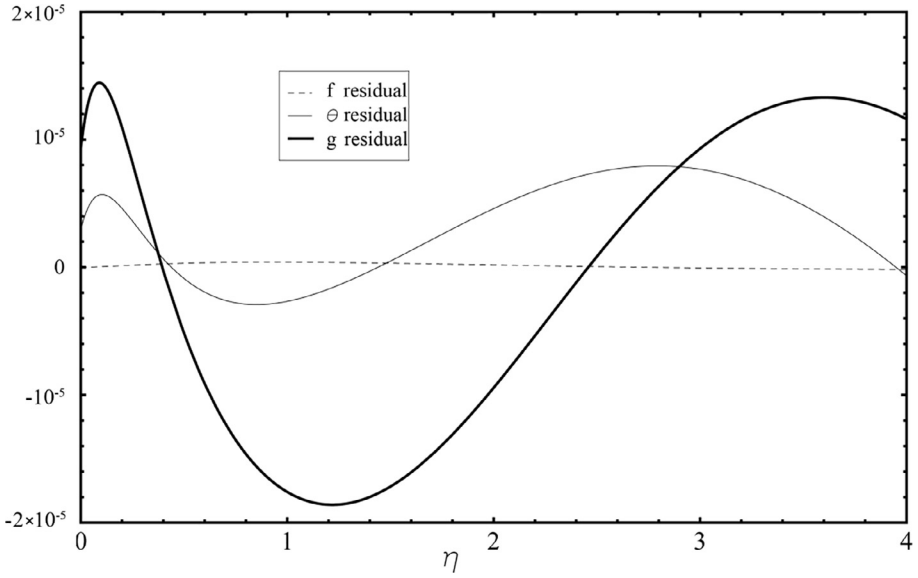

Fig. 4. The residual error for $f(\eta)$, $\theta(\eta)$ and $g(\eta)$ (Eqs. (7), (14) and (18)), for $k_o = 1$ and $m = 1$.

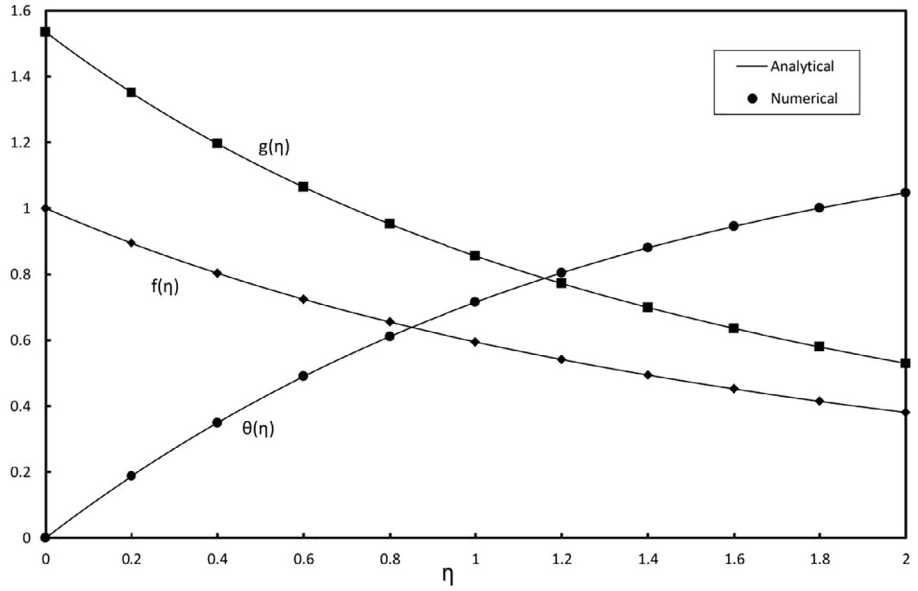

Fig. 5. The Dimensionless stream function $f(\eta)$, temperature $\theta(\eta)$ for PST case and $g(\eta)$ for PHF case in comparison with numerical solution, for $N_R = 2$ and $m = 1$.

$$N_1[\hat{f}\,] = 3\frac{\partial^3\hat{f}\,(\eta;q)}{\partial\eta^3} + 2\hat{f}\,(\eta;q)\frac{\partial^2\hat{f}\,(\eta;q)}{\partial\eta^2} - \left(\frac{\partial\hat{f}\,(\eta;q)}{\partial\eta}\right)^2, \tag{27}$$

$$N_2[\hat{f}\,,\,\hat{\theta}\,] = \frac{\partial^2\hat{\theta}\,(\eta;q)}{\partial\eta^2} + \left(\frac{2k_0Pr}{3}\right)\hat{f}\,(\eta;q)\frac{\partial\hat{\theta}\,(\eta;q)}{\partial\eta} - k_0Prm\hat{\theta}\,(\eta;q)\frac{\partial\hat{f}\,(\eta;q)}{\partial\eta}, \tag{28}$$

$$N_3[\hat{f}\,,\,\hat{g}\,] = \left(\frac{2k_0Pr}{3}\right)\hat{f}\,(\eta;q)\frac{\partial\hat{g}\,(\eta;q)}{\partial\eta} - k_0Pr\left(m+\frac{1}{3}\right)\hat{g}\,(\eta;q)\frac{\partial\hat{f}\,(\eta;q)}{\partial\eta}, \tag{29}$$

where $q \in [0, 1]$ is an embedding parameter and $\hat{f}$, $\hat{\theta}$ and $\hat{g}$ are mapping functions for f, θ and g, respectively. So, the zeroth-order deformation equations are defined as

$$(1-q)L_1[\hat{f}\,(\eta;q) - f_0(\eta)] = qhH_fN_1[\hat{f}\,(\eta;q)], \tag{30}$$

$$(1-q)L_2[\hat{\theta}\,(\eta;q) - \theta_0(\eta)] = qhH_\theta N_2[\hat{f}\,(\eta;q), \hat{\theta}\,(\eta;q)], \tag{31}$$

$$(1-q)L_3[\hat{g}\,(\eta;q) - g_0(\eta)] = qhH_gN_3[\hat{f}\,(\eta;q), \hat{g}\,(\eta;q)], \tag{32}$$

where h is the auxiliary nonzero parameter and H_f, H_θ and H_g are auxiliary functions. The deformation equations are subject to the follow g_0 ing boundary conditions:

$$\hat{f}\,(0;q) = 0, \hat{f}\,'(0;q) = 1, \hat{f}\,'(\infty;q) = 0, \tag{33}$$

$$\hat{\theta}\,(0;q) = 1, \hat{\theta}\,(\infty;q) = 0, \tag{34}$$

$$\hat{g}\,'(0;q) = -1, \hat{g}\,(\infty;q) = 0. \tag{35}$$

When q increases from 0 to 1, $\hat{f}$, $\hat{\theta}$ and $\hat{g}$ vary from initial approximations f_0, θ_0 and to f, θ and g, respectively. Therefore, using Taylor's series expansions, one obtain

$$\hat{f}\,(\eta;q) = f_0(\eta) + \sum_{s=1}^{\infty} f_s(\eta)q^s, \tag{36}$$

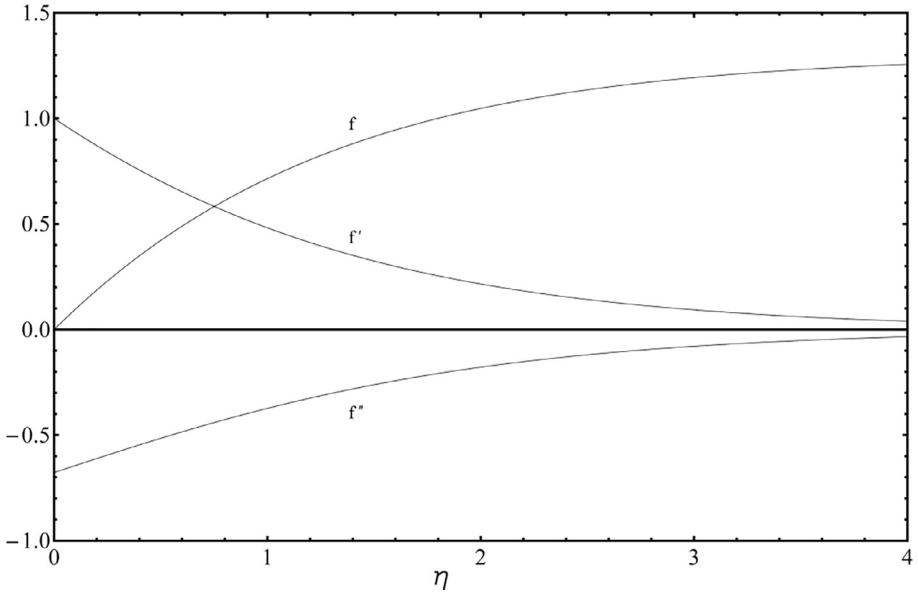

Fig. 6. Dimensionless stream function $f(\eta)$ dimensionless velocity profile $f'(\eta)$ and dimensionless shear stress $f''(\eta)$.

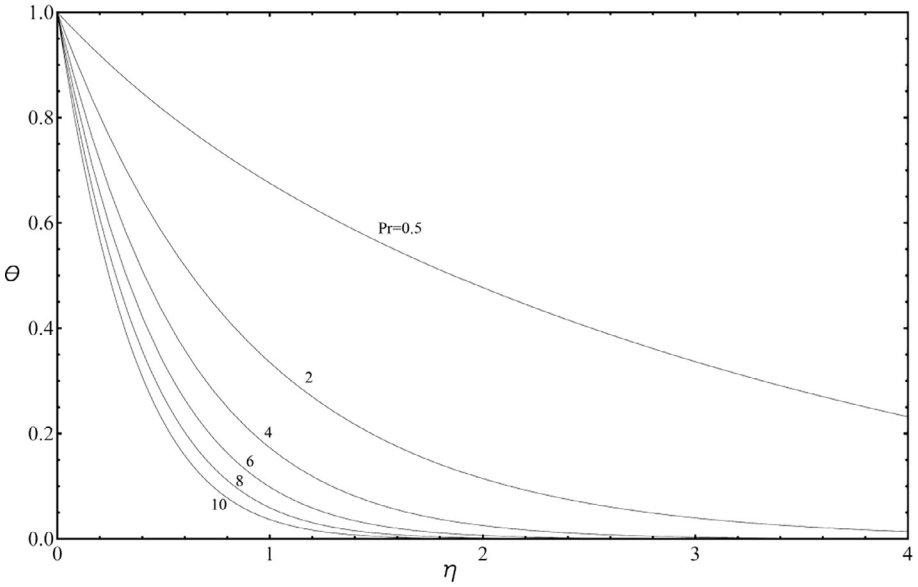

Fig. 7. Dimensionless temperature $\theta(\eta)$ in PST case, for various values of Prandtl number, when $N_R = 2$ and $m = 1$.

$$\hat{\theta}(\eta;q) = \theta_0(\eta) + \sum_{s=1}^{\infty} \theta_s(\eta) q^s, \tag{37}$$

$$\hat{g}(\eta;q) = g_0(\eta) + \sum_{s=1}^{\infty} g_s(\eta) q^s, \tag{38}$$

where

$$\begin{aligned} f_s(\eta) &= \frac{1}{s!}\frac{\partial^s \hat{f}(\eta;q)}{\partial q^s}, \\ \theta_s(\eta) &= \frac{1}{s!}\frac{\partial^s \hat{\theta}(\eta;q)}{\partial q^s}, \; q = 0 \\ g_s(\eta) &= \frac{1}{s!}\frac{\partial^s \hat{g}(\eta;q)}{\partial q^s}, \; q = 0 \end{aligned} \tag{39}$$

Convergence of the series (17)–(19) depends firsthand on the auxiliary parameter h[34]. If h is selected such that series (17)–(19) are convergent at $q = 1$, we have

$$f(\eta) = f_0(\eta) + \sum_{s=1}^{\infty} f_s(\eta), \tag{40}$$

$$\theta(\eta) = \theta_0(\eta) + \sum_{s=1}^{\infty} \theta_s(\eta), \tag{41}$$

$$g(\eta) = g_0(\eta) + \sum_{s=1}^{\infty} g_s(\eta). \tag{42}$$

For s^{th}-order deformation equations, we differentiate zeroth-order deformation equations, and divide each by $s!$ and then set $q = 0$. So the s^{th}-order deformation equations are obtained as follows:

$$L_1[f_s(\eta) - \chi_s f_{s-1}(\eta)] = hH_f R_{1,s}(\eta), \tag{43}$$

$$L_2[\theta_s(\eta) - \chi_s \theta_{s-1}(\eta)] = hH_\theta R_{2,s}(\eta), \tag{44}$$

$$L_3[g_s(\eta) - \chi_s g_{s-1}(\eta)] = hH_g R_{3,s}(\eta), \tag{45}$$

where

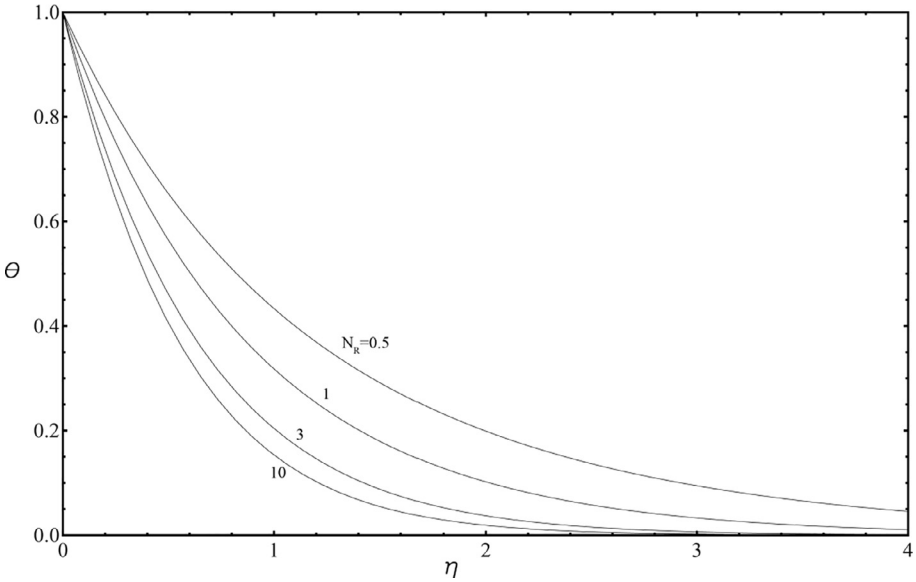

Fig. 8. Dimensionless temperature $\theta(\eta)$ in PST case, for various values of radiation parameter N_R, when $Pr = 3$ and $m = 1$.

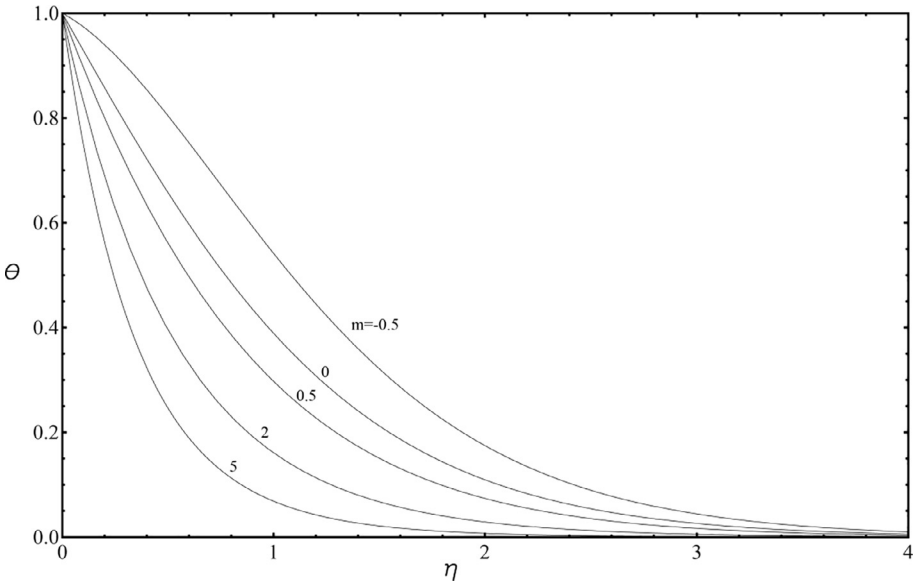

Fig. 9. Dimensionless temperature $\theta(\eta)$ in PST case, for various values of wall temperature parameter m, when $Pr = 3$ and $N_R = 1$.

$$R_{1,s}(\eta) = 3\frac{\partial^3 f_{s-1}(\eta)}{\partial\eta^3} + \sum_{n=0}^{s-1}\left(2f_n(\eta)\frac{\partial^2 f_{s-1-n}(\eta)}{\partial\eta^2} - \frac{\partial f_n(\eta)}{\partial\eta}\frac{\partial f_{s-1-n}(\eta)}{\partial\eta}\right), \tag{46}$$

$$R_{2,s}(\eta) = \frac{\partial^2\theta_{s-1}(\eta)}{\partial\eta^2} + \sum_{n=0}^{s-1}\left(\left(\frac{2k_0Pr}{3}\right)f_n(\eta)\frac{\partial\theta_{s-1-n}(\eta)}{\partial\eta} - k_0Prm\theta_n(\eta)\frac{\partial f_{s-1-n}(\eta)}{\partial\eta}\right), \tag{47}$$

$$R_{3,s}(\eta) = \frac{\partial^2 g_{s-1}(\eta)}{\partial\eta^2} + \sum_{n=0}^{s-1}\left(\left(\frac{2k_0Pr}{3}\right)f_n(\eta)\frac{\partial g_{s-1-n}(\eta)}{\partial\eta} - k_0Pr\left(m+\frac{1}{3}\right)g_n(\eta)\frac{\partial f_{s-1-n}(\eta)}{\partial\eta}\right), \tag{48}$$

$$\chi_s = sign(s-1),\ s \geqslant 1 \tag{49}$$

with the homogenized boundary conditions

$$f_s(0) = 0, f_s'(0) = 0, f_s'(\infty) = 0, \tag{50}$$

$$\theta_s(0) = 0, \theta_s(\infty) = 0, \tag{51}$$

$$g_s'(0) = 0, g_s(\infty) = 0, \tag{52}$$

and the auxiliary functions are

$$H_f = H_g = H_\theta = 1. \tag{53}$$

The system of linear Eqs. (43)–(45) with the boundary conditions (50)–(52) can be solved by means of symbolic software such as MATHEMATICA or Maple. Then, f_s, θ_s and g_s are obtained for $s = 1, 2, \ldots$ as

$$f_1(\eta) = -\frac{2h}{3} - \frac{1}{6}e^{-2\eta h} + \frac{5e^{-\eta h}}{6} + \frac{1}{2}e^{-\eta h}\eta,$$

$$\theta_1(\eta) = \frac{1}{3}e^{-2\eta hPr} - \frac{1}{3}e^{-\eta hPr} - \frac{1}{2}e^{-2\eta hmPr} + \frac{1}{2}e^{-\eta hmPr} - e^{-\eta h}\eta + \frac{2}{3}e^{-\eta hPr}\eta,$$

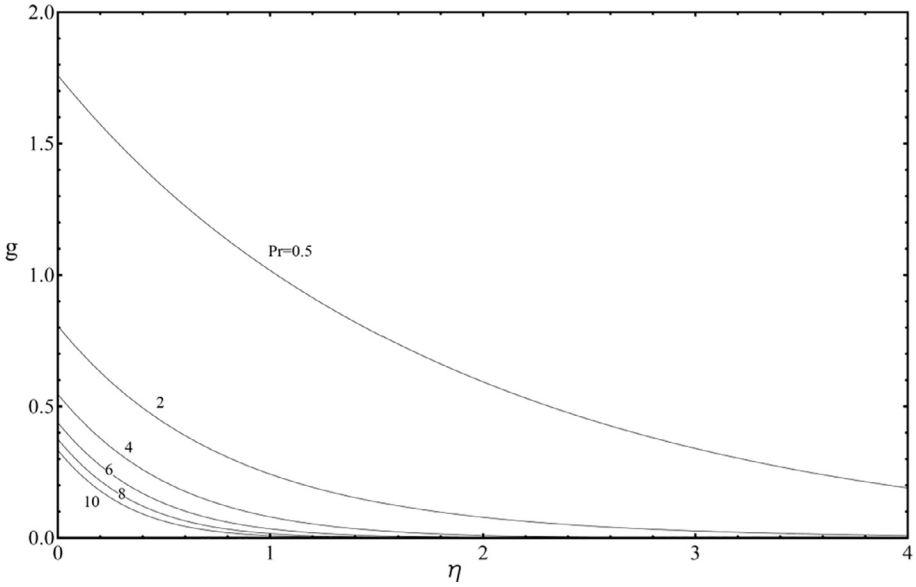

Fig. 10. Dimensionless temperature $g(\eta)$ in PHF case, for various values of Prandtl number, when $N_R = 2$ and $m = 1$.

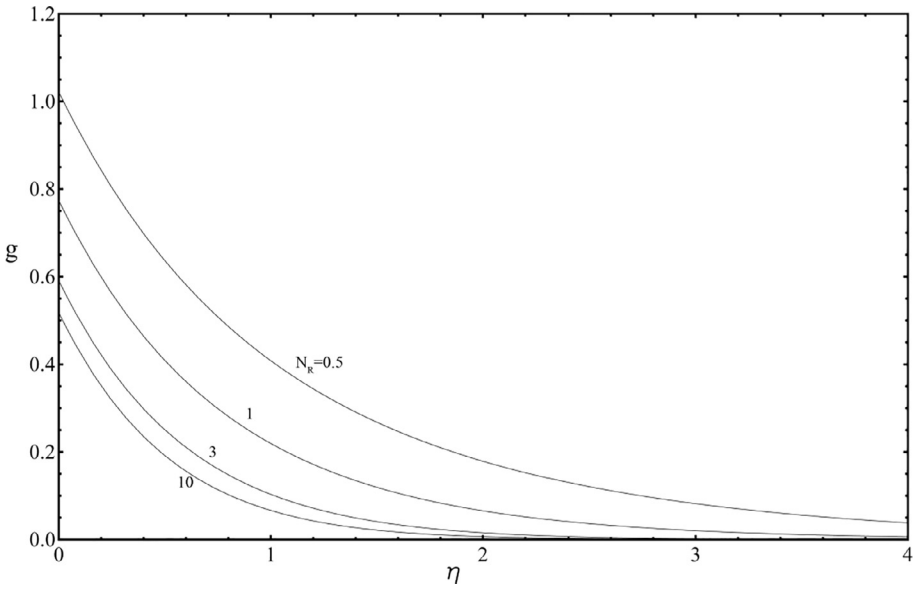

Fig. 11. Dimensionless temperature $g(\eta)$ in PHF case, for various values of radiation parameter N_R, when $Pr = 3$ and $m = 1$.

$$g_1(\eta) = -e^{-\eta h} + \frac{1}{3}e^{-2\eta h}Pr - \frac{1}{2}e^{-2\eta h}(m-\frac{1}{3})Pr + e^{-\eta h}(m-\frac{1}{3})Pr - e^{-\eta h}\eta + \frac{2}{3}e^{-\eta h}Pr,$$

and so on.

Convergence of HAM solutions

The convergence of the series given in the Eqs. (40)–(42) depends on the value of auxiliary parameter h [34]. In order to find the appropriate range of the auxiliary parameter the h-curves of $f''(0)$, $\theta'(0)$ and $g(0)$ are considered, as plotted in Figs. 2 and 3 using twentieth-order of the HAM solution. Upon choosing the appropriate h-value the result is used in the Eqs. (6), (14) and (18) and the solution residual is obtained, that is plotted in Fig. 4. In order to verify the accuracy of the HAM solution, some of the results are compared against the available numerical results. As noted in Fig. 5 an excellent agreement exists between numerical and analytical solutions.

It should be noted that the appropriate range of h values corresponds to the line segments parallel to the h axis in the h plots. This region in h-curves depends on Prandtl number in energy equation, so that increasing the Prandtl number results in a narrower margin for appropriate h values (Figs. 2 and 3). This behavior is due to Prandtl number appearing in the nonlinear terms (Eqs. (14) and (18)). It is also noted in Figs. 2 and 3 that $h = -1$ is out of the permissible range of the auxiliary parameter, so the HPM cannot be used for flow equation, and can be used for energy equation in $Pr = 0$ case only.

Result and discussion

Fig. 6 shows the dimensionless stream function $f(\eta)$, dimensionless velocity profile $f'(\eta)$ and dimensionless shear stress $f''(\eta)$ versus η. It is evident that when the η increases, the dimensionless stream function and dimensionless shear stress increases while dimensionless velocity profile decreases. For the PST case, dimensionless temperature $\theta(\eta)$ is sketched for various values of Prandtl number (Pr), radiation parameter

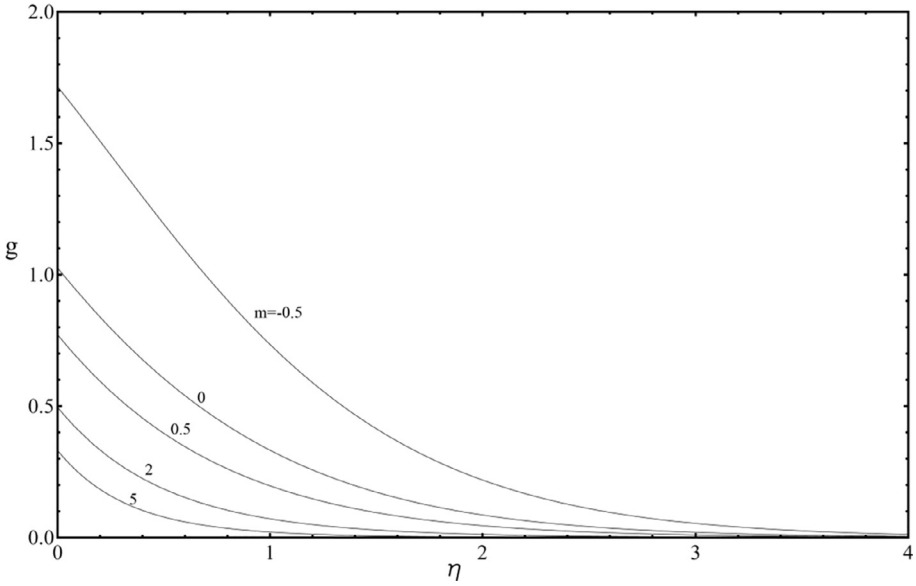

Fig. 12. Dimensionless temperature $g(\eta)$ in PHF case, for various values of wall temperature parameter m, when $Pr = 3$ and $N_R = 1$.

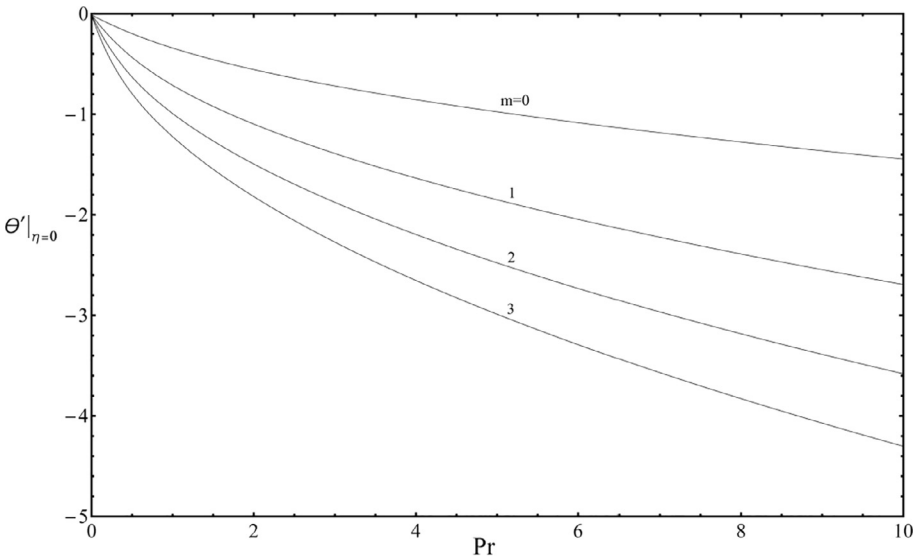

Fig. 13. Effect of Prandtl number on surface heat flux $\theta'(0)$ in PST case for various values of m, when $N_R = 2$.

(N_R) and surface temperature parameter (m) has shown in Figs. 7–9, respectively.

Figs. 7 and 8 show that, as Prandtl number and radiation parameter increases, the dimensionless temperature $\theta(\eta)$ decrease in PST case. According to Fig. 7 ($m = 1$ and $N_R = 2$) by increasing the Prandtl number (when m and N_R are constant), the effects of Prandtl number on $\theta(\eta)$ is decreases. Also, based on Fig. 8 ($m = 1$ and Pr = 3) the effect of N_R on $\theta(\eta)$ decrease, when N_R is increase (by considering constant value for m and Pr). This result qualitatively, agrees with the theory that increase Prandtl number, decrease the heat diffusion and effect of radiation parameter is to decrease of heat transfer to ambient fluid [32]. In fact decreasing the temperature of the fluid due to decrease of the rate of energy transport to the fluid.

Effects of Prandtl number and radiation parameter on dimensionless temperature in PHF case has been shown in Figs. 10 and 11, respectively. According to Fig. 10 ($m = 1$ and $N_R = 2$), the effects of Prandtl number on $g(\eta)$ is decreases when Prandtl number increases (by considering constant value for m and N_R). Fig. 11 shows that if m and Pr is constant (in this figure $m = 1$ and Pr = 3) the effect of N_R on $g(\eta)$ decrease. On the other hand, increase surface temperature parameter m, decrease dimensionless temperature in both PST (Fig. 9) and PHF (Fig. 12) cases.

Effect of Prandtl number on surface heat flux $\theta'(0)$ in PST case and surface temperature $g(0)$ in PHF case for various values of m and constant value for N_R ($N_R = 2$) is shown in Figs. 13 and 14, respectively. Negative values of $\theta'(0)$ implies that, heat flows from the surface to fluid. Figs. 13 and 14 also shows that, by increasing Prandtl number, value of heat flux $|\theta'(0)|$ (in PST case) increases and surface temperature $g(0)$ (in PHF case) decreases in any surface temperature parameter.

Conclusion

In this paper, flow and heat transfer of quiescent fluid over a nonlinearly stretching surface is solved analytically by means of Homotopy Analysis Method (HAM). Convergence of obtained solutions is analyzed and verified by the numerical results. It is shown that HPM method cannot be used for this problem in nonzero values of Prandtl number. Considerable parameters such as dimensionless stream function, velocity and dimensionless temperature in both cases of PST and PHF are represented graphically. The HAM provides a simple solution for both

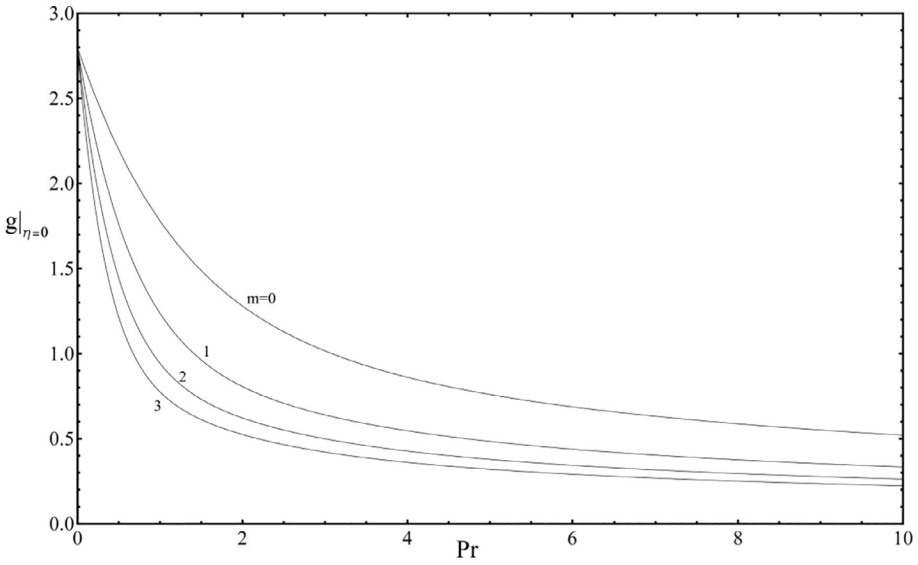

Fig. 14. Effect of Prandtl number on surface temperature $g(0)$ in PHF case for various values of m, when $N_R = 2$.

weakly and strongly nonlinear problem in various values of Prandtl and other parameters and presents a good way to control convergence of solutions by means of auxiliary parameter h.

Appendix A. Supplementary data

Supplementary data associated with this article can be found, in the online version, at http://dx.doi.org/10.1016/j.rinp.2018.05.036.

References

[1] Nejati M, Dimitri R, Tornabene F, Hossein Yas M. Thermal buckling of nano-composite stiffened cylindrical shells reinforced by functionally graded wavy carbon nanotubes with temperature-dependent properties. Appl Sci 2017;7(12):1223.

[2] Yas MH, Nejati M, Jafari SS. Free vibration of functionally graded variable thickness carbon nanotube annular plates. J Comput Methods Eng 2017;35(2):131–58.

[3] Lu DC, Farooq U, Hayat T, Rashidi MM, Ramzan M. Computational analysis of three layer fluid model including a nanomaterial layer. Int J Heat Mass Transf 2018;122:222–8.

[4] Balazadeh N, Sheikholeslami M, Ganji DD, Li Z. Semi analytical analysis for transient Eyring-Powell squeezing flow in a stretching channel due to magnetic field using DTM. J Mol Liq 2018;260:30–6.

[5] Liao SJ. The Proposed Homotopy Analysis Technique for the Solution of Non-Linear Problems. Shanghai Jiao Tong University; 1992.

[6] Liao S. Comparison between the homotopy analysis method and homotopy perturbation method. Appl Math Comput 2005;169(2):1186–94.

[7] Allan FM. Derivation of the Adomian decomposition method using the homotopy analysis method. Appl Math Comput 2007;190(1):6–14.

[8] Rashidi MM, Domairry G, Dinarvand S. Approximate solutions for the Burger and regularized long wave equations by means of the homotopy analysis method. Commun Nonlinear Sci Numer Simul 2009;14(3):708–17.

[9] Liao S. On the homotopy analysis method for nonlinear problems. Appl Math Comput 2004;147(2):499–513.

[10] Liao SJ. A uniformly valid analytic solution of two-dimensional viscous flow over a semi-infinite flat plate. J Fluid Mech 1999;385:101–28.

[11] Liao SJ. An explicit, totally analytic approximate solution for Blasius' viscous flow problems. Int J Non Linear Mech 1999;34(4):759–78.

[12] Liao SJ. On the analytic solution of magnetohydrodynamic flows of non-Newtonian fluids over a stretching sheet. J Fluid Mech 2003;488:189–212.

[13] Jafari SS, Freidoonimehr N. Second law of thermodynamics analysis of hydro-magnetic nano-fluid slip flow over a stretching permeable surface. J Braz Soc Mech Sci Eng 2015;37(4):1245–56.

[14] Jafari SS, Rashidi MM, Johnson S. Analytical approximation of nonlinear vibration of Euler-Bernoulli beams. Latin Am J Solids Struct 2016;13(7):1250–64.

[15] Abbasbandy S. The application of homotopy analysis method to nonlinear equations arising in heat transfer. Phys Lett, Sect A: General, At Solid State Phys 2006;360(1):109–13.

[16] Allan FM, Syam MI. On the analytic solutions of the nonhomogeneous Blasius problem. J Comput Appl Math 2005;182(2):362–71.

[17] Rashidi MM, Erfani E. New analytical method for solving Burgers' and nonlinear heat transfer equations and comparison with HAM. Comput Phys Commun 2009;180(9):1539–44.

[18] Ajam H, Jafari SS, Freidoonimehr N. Analytical approximation of MHD nano-fluid flow induced by a stretching permeable surface using Buongiorno's model. Ain Shams Eng J 2016.

[19] Abbasbandy S. Homotopy analysis method for heat radiation equations. Int Commun Heat Mass Transfer 2007;34(3):380–7.

[20] Marinca V, Herişanu N. Application of Optimal Homotopy Asymptotic Method for solving nonlinear equations arising in heat transfer. Int Commun Heat Mass Transfer 2008;35(6):710–5.

[21] Sheikholeslami M, Jafaryar M, Bateni K, Ganji DD. Two phase modeling of nano-fluid flow in existence of melting heat transfer by means of HAM. Indian J Phys 2018;92(2):205–14.

[22] Char MI. Heat and mass transfer in a hydromagnetic flow of the viscoelastic fluid over a stretching sheet. J Math Anal Appl 1994;186(3):674–89.

[23] Cortell R. Numerical solutions for the flow of a fluid of grade three past an infinite porous plate. Int J Non Linear Mech 1993;28(6):623–6.

[24] Cortell R. Similarity solutions for flow and heat transfer of a viscoelastic fluid over a stretching sheet. Int J Non Linear Mech 1994;29(2):155–61.

[25] Cortell R. MHD boundary-layer flow and heat transfer of a non-Newtonian power-law fluid past a moving plate with thermal radiation. Nuovo Cimento B Serie 2006;121(9):951–64.

[26] Prasad KV, Abel MS, Khan SK. Momentum and heat transfer in visco-elastic fluid flow in a porous medium over a non-isothermal stretching sheet. Int J Numer Meth Heat Fluid Flow 2000;10(8):786–801.

[27] Prasad KV, Abel MS, Khan SK, Datti PS. Non-Darcy forced convective heat transfer in a viscoelastic fluid flow over a nonisothermal stretching sheet. J Porous Media 2002;5(1):41–7.

[28] Chen CH. Convection cooling of a continuously moving surface in manufacturing processes. J Mater Process Technol 2003;138(1-3):332–8.

[29] Vajravelu K. Viscous flow over a nonlinearly stretching sheet. Appl Math Comput 2001;124(3):281–8.

[30] Ali ME. On thermal boundary layer on a power-law stretched surface with suction or injection. Int J Heat Fluid Flow 1995;16(4):280–90.

[31] Elbashbeshy EMA. Heat transfer over an exponentially stretching continuous surface with suction. Arch Mech 2001;53(6):643–51.

[32] Rafael Cortell B. Similarity solutions for flow and heat transfer of a quiescent fluid over a nonlinearly stretching surface. J Mater Process Technol 2008;203(1-3):176–83.

[33] Siddheshwar PG, Mahabaleswar US. Effects of radiation and heat source on MHD flow of a viscoelastic liquid and heat transfer over a stretching sheet. Int J Non Linear Mech 2005;40(6):807–20.

[34] Liao SJ. Beyond Perturbation: Introduction to the Homotopy Analysis Method. 2003, Boca Raton: Beyond Perturbation: Introduction to the Homotopy Analysis Method.